IEEJ TRANSACTIONS ON ELECTRICAL AND ELECTRONIC ENGINEERING
IEEJ Trans 2015; **10**(s1): S34–S41
Published online in Wiley Online Library (wileyonlinelibrary.com). DOI:10.1002/tee.22162

Paper

Real-Time Calculation of Power System Bus Voltage Using a Hybrid Approach Combining the Newton–Raphson Method and Dynamic Programming

Wei-Tzer Huang[a], Non-member
Kai-Chao Yao, Non-member
Chun-Ching Wu, Non-member

The calculation of the magnitudes and phase angles of the bus voltage is a challenging task in real-time applications for power systems. Voltage profile, which denotes the present conditions of a power system, is determined by executing the traditional AC power flow program or by searching the supervisory control and data acquisition system. The AC power flow program is not suitable for several real-time applications, such as contingency analysis and security control calculations, because of its complexity and convergence problems. Fast computation is the major concern in such applications. In this paper, a new method based on sensitivity factors, referred to as Jacobian-based distribution factors (JBDFs), is proposed for calculating the magnitudes and phase angles of bus voltages. This method requires setting up JBDFs and deriving optimal solution paths of bus voltage for non-swing buses through dynamic programming under base-case loading conditions. Under real-time conditions, the proposed method initially calculates real and reactive power line flows via JBDFs, and then computes the voltage magnitudes and phase angles of non-swing buses through the derived optimal solution paths. The excellence of the proposed hybrid calculation method is verified by IEEE test systems. Simulation results demonstrate that the proposed method exhibits fast computation and high accuracy. Thus, the method is suitable for real-time applications. © 2015 Institute of Electrical Engineers of Japan. Published by John Wiley & Sons, Inc.

Keywords: bus voltage, sensitivity factors, Newton–Raphson method, dynamic programming, optimal path, real-time application

Received 23 November 2014; Revised 30 March 2015

1. Introduction

The power flow program in an AC power system can be modeled by a set of nonlinear equations and solved by numerical iterative methods. The well-known solution approaches are the Gauss–Seidel [1], Newton–Raphson [1,2], fast decoupled methods [3], and new, efficient iterative techniques [4–7]. However, in practical large-scale power systems consisting of thousands of buses, the standard Newton–Raphson method has a slow execution time, because of the need for recalculation of a large Jacobian matrix in each iteration. Therefore, the fast decoupled power flow approaches were presented to overcome this disadvantage, and it is very useful in practical power system analyses, such as contingency analysis, online power flow control, etc. Nevertheless, the aforementioned methods still require numerous iterations for convergence. Approaches based on network sensitivity, such as generation shift distribution factor (GSDF) [8], generalized generation distribution factor (GGDF) [9], Z-bus distribution factor (ZBD) [10], and power transfer distribution factor [11,12], have been proposed for improving the weakness of conventional methods. Although the aforementioned sensitivity factors still have disadvantages, their calculation time is small and they do not need any iteration after the load demand is changed. Therefore, these factors are adopted in economic dispatching [13], optimal power flow, security control [14], and line flow computation after a fault occurs.

In [15], a Jacobian-based distribution factor (JBDF) is proposed for overcoming the shortcomings of GSDF, GGDF, and ZBD. The correlative partial differential terms of JBDF are derived according to base-case power flow solutions and the inverse Jacobian matrix. Then, the active and reactive power JBDF terms are established [15]. This approach reflects changes in the complex injection power. Changes in load conditions from base-case loads, with either conforming or nonconforming changes in complex power in each bus, can be used to compute active and reactive power flows without iterations, rapidly. The use of JBDF for solving line flow after a change in load demand is fine except for solving the magnitude and phase angle of bus voltage. In this paper, both line flow and the bus voltage can be solved by the proposed hybrid approach based on sensitivity factors. Consequently, the Newton–Raphson method is employed as the base-case solution framework. The essential difference is that the proposed approach computes solutions of the bus voltage equations via JBDF bus voltage formulas instead of iterative nonlinear equations. Figure 1 shows the schematic diagram of the proposed approach and its real-time applications for modern power systems. This approach can simplify the solution procedure. With this simplification, a reduction in the overall execution time is expected. Thus, the proposed approach, which combines the Newton–Raphson method and dynamic programming, is a fast and effective soft calculation method for real-time applications of power systems. The rest of the paper is organized as follows. Section 2 presents the derivation of the JBDF bus voltage formulas. Section 3 describes the solution procedure. Section 4 discusses the numerical results. Section 5 concludes the paper.

[a] Correspondence to: Wei-Tzer Huang.
E-mail: vichuang@cc.ncue.edu.tw

Department of Industrial Education and Technology, National Changhua University of Education, No. 2 Shida Road, Changhua 500, Taiwan, Republic of China

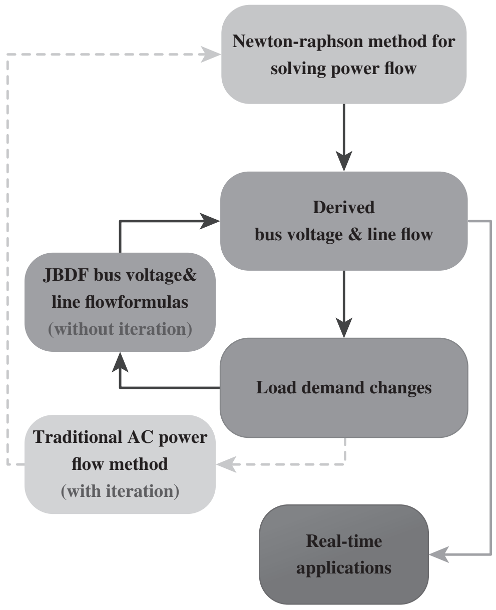

Fig. 1. Schematic diagram of the proposed approach

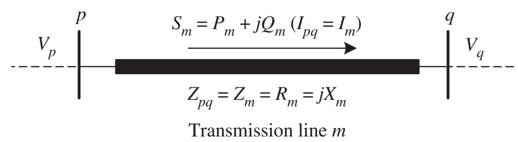

Fig. 2. Equivalent circuit model of a transmission line

2. Derivation of the JBDF Bus Voltage Formulas

The proposed hybrid approach initially computes the real-time line flow solution using the JBDF method based on the base-case power flow solution of the Newton–Raphson method after load demand changes across all buses. Then, the voltage magnitudes and phase angles of the non-swing buses are calculated using the JBDF bus voltage formulas derived from the optimal paths obtained via dynamic programming. Consequently, the voltage magnitudes and phase angles of the system buses can be solved rapidly and correctly without any iteration. An object function, which is composed of line voltage drop, must be established and then solved by dynamic programming to address possible multiple solution paths from the swing bus to the other buses, including PV and PQ [16–18]. The optimal paths from the swing bus to the other buses in this section are obtained in advance according to the base-case power flow solution. These paths can also be used for solving real-time voltage magnitudes and phase angles of non-swing buses.

2.1. Formula derivation Following [15], the active and reactive power flows of line m can be modeled as base-case active and reactive power flows (P_m^0, Q_m^0) plus the summation of the production of JBDF as well as incremental active and reactive power injections. The derivation of (1)–(6) are shown in the Appendix.

$$P_m \cong P_m^0 + \sum_{i=1}^{NB} F_p(m,i)\Delta P_i + \sum_{i=1}^{NB} K_p(m,i)\Delta Q_i \tag{1}$$

$$Q_m \cong Q_m^0 + \sum_{i=1}^{NB} F_q(m,i)\Delta P_i + \sum_{i=1}^{NB} K_q(m,i)\Delta Q_i \tag{2}$$

where $F_p(m,i)$, $K_p(m,i)$, $F_q(m,i)$, and $K_q(m,i)$ represent the active and reactive power JBDFs; besides, NB denotes the bus number of the system; ΔP_i and ΔQ_i represent the increments of active and reactive power in bus i. These factors can be derived as follows:

$$\begin{aligned} F_p(m,i) = {} & \left(\frac{\partial|V_p|}{\partial P_i}\right)\cdot\frac{\partial P_m}{\partial|V_p|} + \left(\frac{\partial|V_q|}{\partial P_i}\right)\cdot\frac{\partial P_m}{\partial|V_q|} \\ & + \left(\frac{\partial\delta_p}{\partial P_i}\right)\cdot\frac{\partial P_m}{\partial\delta_p} + \left(\frac{\partial\delta_q}{\partial P_i}\right)\cdot\frac{\partial P_m}{\partial\delta_q} \end{aligned} \tag{3}$$

$$\begin{aligned} K_p(m,i) = {} & \left(\frac{\partial|V_p|}{\partial Q_i}\right)\frac{\partial P_m}{\partial|V_p|} + \left(\frac{\partial|V_q|}{\partial Q_i}\right)\frac{\partial P_m}{\partial|V_q|} \\ & + \left(\frac{\partial\delta_p}{\partial Q_i}\right)\frac{\partial P_m}{\partial\delta_p} + \left(\frac{\partial\delta_q}{\partial Q_i}\right)\frac{\partial P_m}{\partial\delta_q} \end{aligned} \tag{4}$$

$$\begin{aligned} F_q(m,i) = {} & \left(\frac{\partial|V_p|}{\partial P_i}\right)\cdot\frac{\partial Q_m}{\partial|V_p|} + \left(\frac{\partial|V_q|}{\partial P_i}\right)\cdot\frac{\partial Q_m}{\partial|V_q|} \\ & + \left(\frac{\partial\delta_p}{\partial P_i}\right)\cdot\frac{\partial Q_m}{\partial\delta_p} + \left(\frac{\partial\delta_q}{\partial P_i}\right)\cdot\frac{\partial Q_m}{\partial\delta_q} \end{aligned} \tag{5}$$

$$\begin{aligned} K_q(m,i) = {} & \left(\frac{\partial|V_p|}{\partial Q_i}\right)\frac{\partial Q_m}{\partial|V_p|} + \left(\frac{\partial|V_q|}{\partial Q_i}\right)\frac{\partial Q_m}{\partial|V_q|} \\ & + \left(\frac{\partial\delta_p}{\partial Q_i}\right)\frac{\partial Q_m}{\partial\delta_p} + \left(\frac{\partial\delta_q}{\partial Q_i}\right)\frac{\partial Q_m}{\partial\delta_q} \end{aligned} \tag{6}$$

The active and reactive power line flows of each line section can be obtained with a high degree of accuracy without risking divergence by using the previously described JBDF method.

In Fig. 2, S_m, P_m, and Q_m represent the complex, active, and reactive power line flows of line m, respectively. The current of line m can be represented as

$$I_m = \frac{P_m - jQ_m}{V_p^*} \tag{7}$$

where V_p^* denotes the conjugate of voltage at bus p. In practical power systems, any changes in bus power injection cause variations in all bus voltage magnitudes and phase angles. Therefore, substituting (1) and (2) for P_m and Q_m in (7) will yield

$$\begin{aligned} I_m = {} & \frac{P_m^0 + \sum_{i=1}^{NB} F_p(m,i)\Delta P_i + \sum_{i=1}^{NB} K_p(m,i)\Delta Q_i}{V_p^*} \\ & -j\,\frac{Q_m^0 + \sum_{i=1}^{NB} F_q(m,i)\Delta P_i + \sum_{i=1}^{NB} K_q(m,i)\Delta Q_i}{V_p^*} \end{aligned} \tag{8}$$

Following Ohm's law, the voltage drop of line m from bus p to bus q can be expressed as

$$V_{pq} = I_m \cdot Z_m \tag{9}$$

where Z_m denotes the primitive line impedance of line m, and V_{pq} denotes the voltage drop of line m. The voltage magnitudes and phase angles of non-swing buses can be derived from the calculations of the voltage drop of all line sections.

2.2. Illustration of the proposed algorithm A five-bus sample system is shown in Fig. 3. This system is used to illustrate the solution procedure of the proposed approach. Bus 1 is set as the swing bus, and the bus voltage is V_1. According to the JBDF and base-case power flow solution, the currents in each line section can be derived and expressed as follows:

$$I_1 = \frac{1}{V_1^*}\cdot\left\{\begin{aligned} & P_1^0 + \sum_{i=1}^{5}[F_p(1,i)\Delta P_i + K_p(1,i)\Delta Q_i] \\ & -j\left[Q_1^0 + \sum_{i=1}^{5}[F_q(1,i)\Delta P_i + K_q(1,i)\Delta Q_i]\right] \end{aligned}\right\} \tag{10}$$

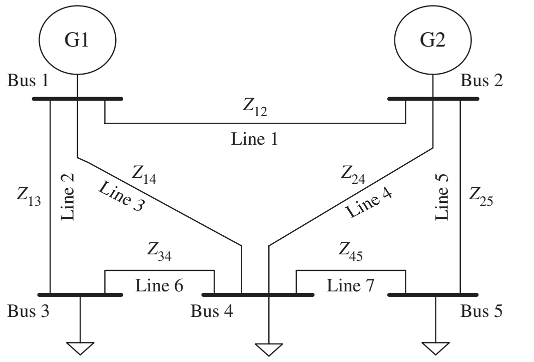

Fig. 3. Five-bus sample system

$$I_2 = \frac{1}{V_1^*} \cdot \left\{ \begin{array}{l} P_2^0 + \sum_{i=1}^{5} [F_p(2,i)\Delta P_i + K_p(2,i)\Delta Q_i] \\ \quad -j\left[Q_2^0 + \sum_{i=1}^{5} [F_q(2,i)\Delta P_i + K_q(2,i)\Delta Q_i] \right] \end{array} \right\} \quad (11)$$

$$I_3 = \frac{1}{V_1^*} \cdot \left\{ \begin{array}{l} P_3^0 + \sum_{i=1}^{5} [F_p(3,i)\Delta P_i + K_p(3,i)\Delta Q_i] \\ \quad -j\left[Q_3^0 + \sum_{i=1}^{5} [F_q(3,i)\Delta P_i + K_q(3,i)\Delta Q_i] \right] \end{array} \right\} \quad (12)$$

$$I_4 = \frac{1}{V_1^*} \cdot \left\{ \begin{array}{l} P_4^0 + \sum_{i=1}^{5} [F_p(4,i)\Delta P_i + K_p(4,i)\Delta Q_i] \\ \quad -j\left[Q_4^0 + \sum_{i=1}^{5} [F_q(4,i)\Delta P_i + K_q(4,i)\Delta Q_i] \right] \end{array} \right\} \quad (13)$$

$$I_5 = \frac{1}{V_1^*} \cdot \left\{ \begin{array}{l} P_5^0 + \sum_{i=1}^{5} [F_p(5,i)\Delta P_i + K_p(5,i)\Delta Q_i] \\ \quad -j\left[Q_5^0 + \sum_{i=1}^{5} [F_q(5,i)\Delta P_i + K_q(5,i)\Delta Q_i] \right] \end{array} \right\} \quad (14)$$

$$I_6 = \frac{1}{V_1^*} \cdot \left\{ \begin{array}{l} P_6^0 + \sum_{i=1}^{5} [F_p(6,i)\Delta P_i + K_p(6,i)\Delta Q_i] \\ \quad -j\left[Q_6^0 + \sum_{i=1}^{5} [F_q(6,i)\Delta P_i + K_q(6,i)\Delta Q_i] \right] \end{array} \right\} \quad (15)$$

$$I_7 = \frac{1}{V_1^*} \cdot \left\{ \begin{array}{l} P_7^0 + \sum_{i=1}^{5} [F_p(7,i)\Delta P_i + K_p(7,i)\Delta Q_i] \\ \quad -j\left[Q_7^0 + \sum_{i=1}^{5} [F_q(7,i)\Delta P_i + K_q(7,i)\Delta Q_i] \right] \end{array} \right\} \quad (16)$$

In addition, the voltage drop in each line section can be expressed as follows:

$$V_1 - V_2 = V_{12} = I_1 Z_{12} \quad (17)$$

$$V_1 - V_3 = V_{13} = I_2 Z_{13} \quad (18)$$

$$V_1 - V_4 = V_{14} = I_3 Z_{14} \quad (19)$$

$$V_2 - V_4 = V_{24} = I_4 Z_{24} \quad (20)$$

$$V_2 - V_5 = V_{25} = I_5 Z_{25} \quad (21)$$

$$V_3 - V_4 = V_{34} = I_6 Z_{34} \quad (22)$$

$$V_4 - V_5 = V_{45} = I_7 Z_{45} \quad (23)$$

The non-swing bus voltage can be derived from (17)–(23) and the known bus voltage $V_1 = 1.0\angle 0^\circ$ pu, as follows:

$$V_2 = V_1 - V_{12} = V_1 - I_1 Z_{12} \quad (24)$$

$$V_3 = V_1 - V_{13} = V_1 - I_2 Z_{13} \quad (25)$$

$$V_4 = V_1 - V_{14} = V_1 - I_3 Z_{14} \quad (26)$$

where,V_4 can also be derived by the other circuit path, that is

$$V_4 - V_5 = V_{45} = I_7 Z_{45} \quad (27)$$

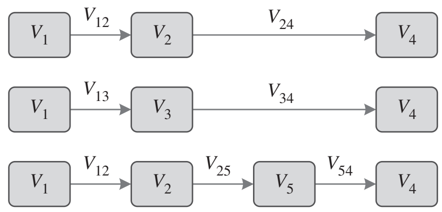

Fig. 4. Bus voltage solution path between bus 1 and bus 4 of the five-bus sample system

Furthermore, the voltage at bus 4 can be rewritten as

$$V_4 = V_2 - V_{24} = V_2 - I_4 Z_{24} = V_1 - V_{12} - V_{24} \quad (28)$$

or

$$V_4 = V_3 - V_{34} = V_3 - I_6 Z_{34} = V_3 - V_{13} - V_{34} \quad (29)$$

or

$$V_4 = V_1 - V_{12} - V_{25} - V_{54} \quad (30)$$

Additionally, V_5 can be derived from bus 1 to bus 5 through bus 2. Therefore

$$V_5 = V_1 - V_{12} - V_{25} \quad (31)$$

V_5 can also be derived through the other circuit path as follows:

$$V_5 = V_1 - V_{12} - V_{24} - V_{45} \quad (32)$$

or

$$V_5 = V_1 - V_{13} - V_{34} - V_{45} \quad (33)$$

The derivation results show that numerous solution paths exist between the swing and non-swing buses. For example, Fig. 4 shows three solution paths that can be used to find the voltage at bus 4: bus 1–bus 2–bus 4, bus 1–bus 3–bus 4, and bus1–bus 2–bus 5–bus 4. Therefore, there are two approaches, which are the brute force and dynamic programming methods, to calculate the voltage at bus 4. However, the error of the bus voltage solution by the computing approach mentioned above resulted from the current I_{pq}(as shown in Fig. 2) in $I_{pq}Z_{pq}$ according to the error propagation principle. Thus, the optimal solution path is chosen by minimizing the summation of $I_{pq}Z_{pq}$. Consequently, this problem is similar to the minimum cost problem unit comment by the dynamic programming method. In this paper, the dynamic programming algorithm is used to find the optimal path for calculating the bus voltage. Because the system topology is formed by the elements and their connections, each power system has its unique circuit topology. Therefore, there are different paths from the swing bus to each end buses, and each path is composed of the interconnected branches (transmission lines) and buses, in which the feasible bus represents the bus in the path, which is from the swing bus to end bus; otherwise, the bus that is not in the path means infeasible bus, as shown in Fig.5. Consequently, in the dynamic-programming-based bus voltage calculation algorithm, for each circuit path, different combinations of buses and branches, which render feasible solutions to the minimum voltage drop path problem, are considered. At each line section, the derived JBDF bus voltage formulas are applied on every feasible connection to calculate the voltage drops. At each bus, a pointer is assigned to every feasible connection that uniquely identifies its predecessor, yielding the least cumulative voltage drop. The optimal solution path is obtained by tracing the circuit path linking the successive decisions that rendered the least total cumulative voltage drop. In this paper, the forward dynamic programming must

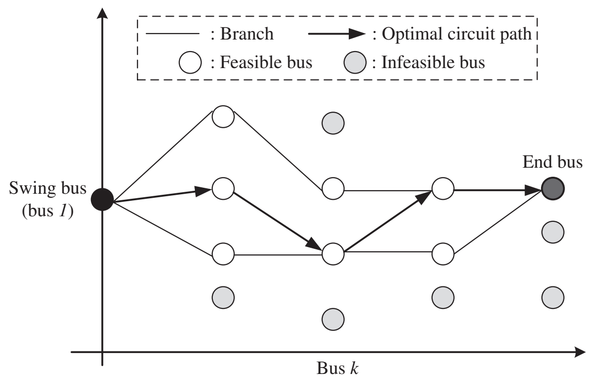

Fig. 5. Dynamic programming of optimal circuit path of minimum voltage drop

be used. The recursion function required to solve this problem is given by

$$CVD_{pq} = \min\left[I_{pq}Z_{pq} + \sum_{b=1}^{n} VD_{p-1,q-1}\right] \tag{34}$$

where $CVD_{pq} = \sum_{b=1}^{n} VD_{p,q}$ is the cumulative voltage drop associated with bus p to bus q, for all buses from bus $p-1$ to bus $q-1$.

To sum up, the optimal solution paths between swing and non-swing buses can be found and established in base-case or off-line stages. Then, the voltage magnitudes and phase angles of non-swing buses can be solved using the paths established after system load demand changes for real-time applications.

3. Solution Procedure

The proposed hybrid approach involves the Newton–Raphson method, JBDF sensitivity factors, and dynamic programming. Except for the base-case power flow solution by the Newton–Raphson method, line flow and bus voltage will be solved by JBDF sensitivity factors and dynamic programming after system load demand changes for real-time applications. The solution flowchart for real-time applications is shown in Fig. 6. This flowchart can also be organized by the following steps.

Step 1: The base-case power flow is calculated using the Newton–Raphson method. The active and reactive power line flows, as well as the bus voltages, are obtained.

Step 2: Dynamic programming is used to build optimal solution paths from the swing bus to the end bus.

Step 3: Line flow JBDF formulas for calculating active and reactive power line flows after load demand changes are used.

Step 4: Bus voltage JBDF formulas as well as the established optimal solution paths for computing bus voltage magnitudes and phase angles after load demand changes are used.

Finally, the proposed approach is tested using the IEEE 14-bus, 25-bus, and 30-bus test systems to verify its accuracy compared with the exact solution provided by the traditional AC power flow method (Newton–Raphson method).

4. Discussion and Analysis of the Numerical Results

The mathematical models and solution procedure of the proposed approach for calculating line flow and bus voltage were derived in Sections 2 and 3. The proposed approach was coded using MATLAB and executed on a Windows XP-based Intel Pentium-M 2.0 GHz CPU personal computer based on the aforementioned formulations. The performance of the approach was assessed according to standard IEEE test systems [19].

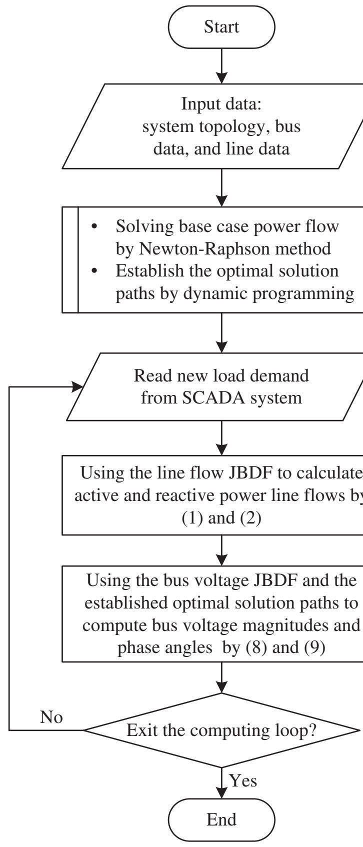

Fig. 6. Flowchart of the proposed hybrid method

4.1. Test systems The single-line diagram, line data, and bus data of the IEEE test systems for steady-state modeling and simulation are listed in [19]. In the present study, only the numerical results of the IEEE 30-bus test system are analyzed and discussed in detail to verify the accuracy of the proposed approach. The results of the other test systems, namely IEEE 14-bus and 25-bus, are used to discuss and compare the maximum errors and execution time.

4.2. Optimal solution paths The IEEE 30-bus test system with medium-scale power has 30 buses and 60 transmission lines. The optimal solution paths are shown in Fig. 7, which means the minimum voltage drop circuit paths between swing and non-swing buses are obtained by dynamic programming. For example, numerous paths can be taken from bus 1 to bus 30; however, only one minimum line voltage drop path exists (Fig. 7). This path is optimal because it contains the least errors among all paths. Consequently, the voltage magnitude and phase angle at bus 30 can be solved by the path bus 1–bus 2–bus 6-bus 28–bus 27–bus 30. Therefore, V_{30} can be calculated through V_1-V_{12}-V_{26}-$V_{2,28}$-$V_{28,27}$-$V_{27,30}$ using (1)–(9).

4.3. Numerical results The developed sensitivity-based approaches, such as GSDF and GGDF [8,9] cannot deal with the conforming load demand change; however, the ZBD [10] and JBDF [15] are able to cope with both the conforming and nonconforming load demand changes. Consequently, three scenarios are assumed in this paper: two conforming and one nonconforming load changes in system demand from the base load. The conforming load change means that the system load increase or decrease is the same in all buses; however, the nonconforming load change means that the system load increase or decrease is randomly in all buses; this scenario is close to reflecting the characteristics of changes in system demand for

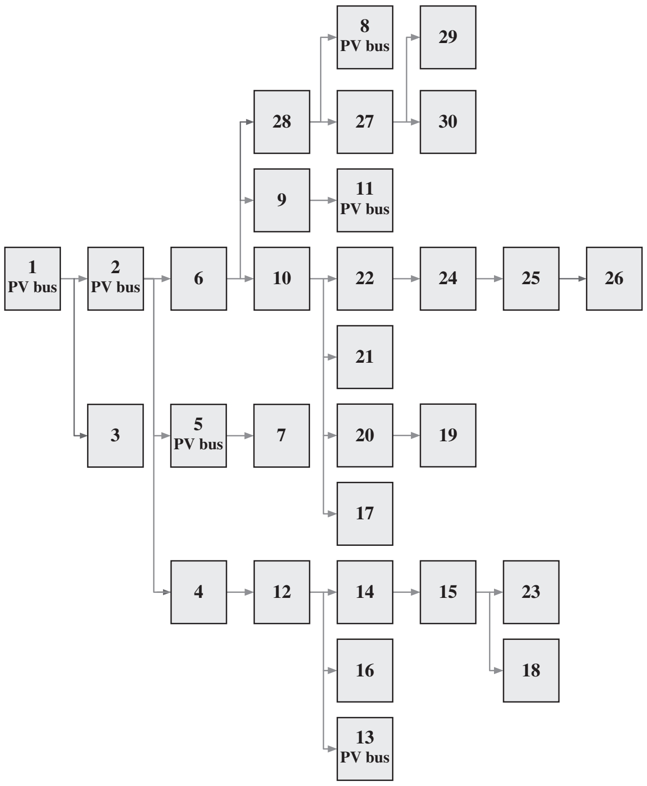

Fig. 7. Bus voltage optimal solution paths of the IEEE 30-bus test system

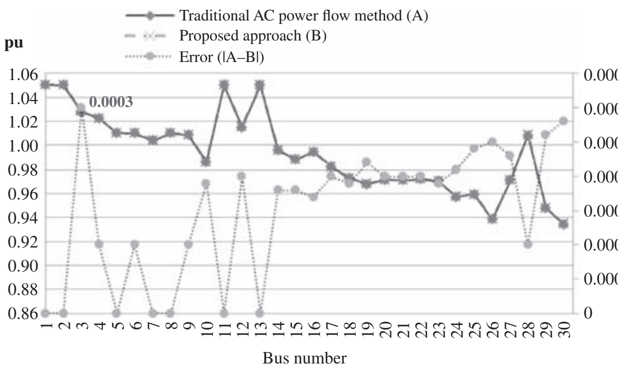

Fig. 8. Numerical results of the voltage magnitude of the conforming load demand with 10% increase

practical systems. The numerical results of the voltage magnitudes and phase angles as the conforming load demand increased by 10% are shown in Figs 8 and 9, respectively. Figure 8 shows that the maximum voltage magnitude mismatch of the proposed approach is 0.0003 pu at bus 3 and that the maximum percentage error is 0.0292%. Figure 9 shows that the maximum phase angle mismatch of the proposed approach is 0.0091° at bus 29 and that the maximum percentage error is 0.1249%. Similarly, the numerical results of the voltage magnitudes and phase angles as the conforming load demand increased by 20% are shown in Figs 10 and 11, respectively. Figure 10 shows that the maximum voltage magnitude mismatch of the proposed approach is 0.0011 pu at bus 30 and that the maximum percentage error is 0.1222%. Figure 11 shows that the maximum phase angle mismatch of the proposed approach is 0.0390° at bus 30 and that the maximum percentage error is 0.3234%. For the nonconforming load demand change, the assumption of the percentage changes in the nonconforming load demand is listed in Table I. The simulation results in Fig. 12 show that the maximum voltage magnitude mismatch of the proposed

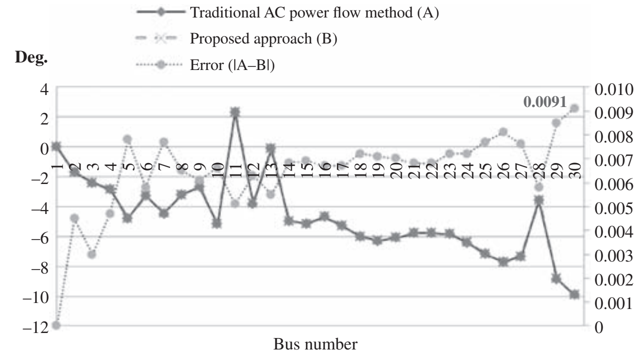

Fig. 9. Numerical results of the phase angle of the conforming load demand with 10% increase

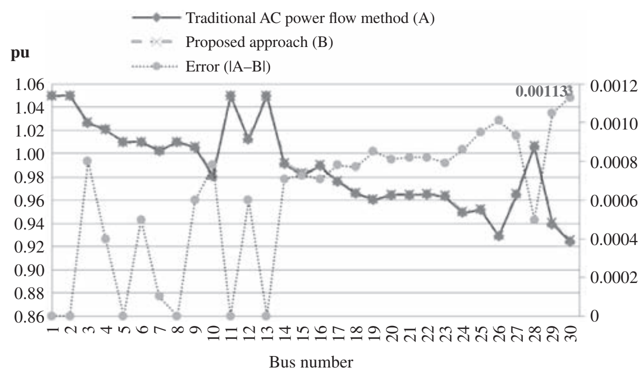

Fig. 10. Numerical results of the voltage magnitude of the conforming load demand with 20% increase

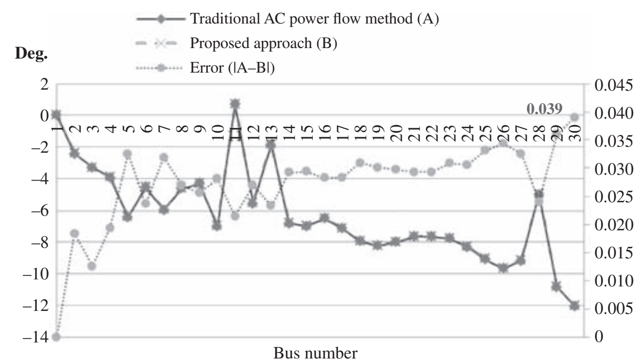

Fig. 11. Numerical results of the phase angle of the conforming load demand with 20% increase

approach is 0.0003 pu at bus 19 and that the maximum percentage error is 0.0353%. Besides, Fig. 13 shows that the maximum phase angle mismatch of the proposed approach is 0.0075° at bus 18 and that the maximum percentage error is 0.1271%. According to the simulation results, although the acceptable errors of bus voltage are obtained by the proposed approach without any iteration, it is certain that the efficiency is absolutely better than the traditional AC power flow method with iteration. Consequently, our method can be applied for real-time applications.

4.4. Discussion The numerical results indicate minimal errors in the voltage magnitude and phase angle of the IEEE 30-bus test system. Moreover, three IEEE test systems were used to examine the maximum errors in the bus voltage of the proposed approach. The results indicate that the maximum errors are small, as shown in Table II. Furthermore, Table III shows that the execution time of the proposed approach is superior to that

Table I. Percentage of nonconforming system demands

% \ Bus number	**1**	**2**	**3**	**4**	**5**	**6**	**7**	**8**	**9**	**10**
ΔP_i	0	0	15	25	0	18	6	0	5	24
ΔQ_i	0	0	10	30	0	8	25	0	20	14
% \ Bus number	**11**	**12**	**13**	**14**	**15**	**16**	**17**	**18**	**19**	**20**
ΔP_i	0	28	0	0	5	30	15	6	30	11
ΔQ_i	0	18	0	6	27	30	12	5	7	6
% \ Bus number	**21**	**22**	**23**	**24**	**25**	**26**	**27**	**28**	**29**	**30**
ΔP_i	7	15	12	0	16	11	30	14	25	0
ΔQ_i	23	6	25	16	6	22	28	24	5	10

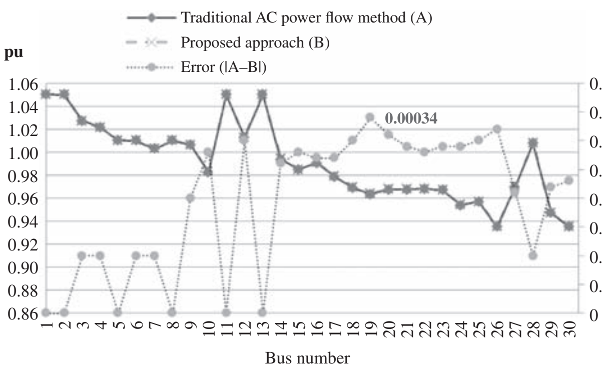

Fig. 12. Numerical results of the voltage magnitude of the nonconforming load demand change

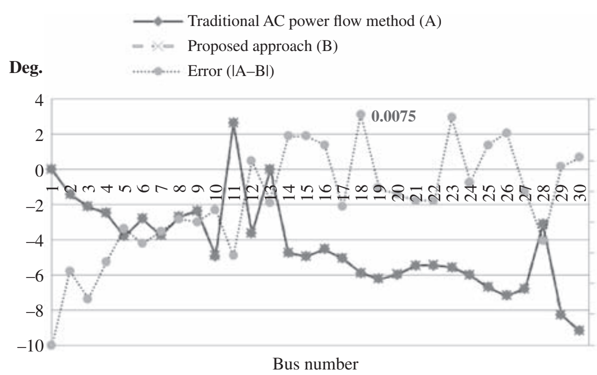

Fig. 13. Numerical results of the phase angle of the nonconforming load demand change

of the traditional AC power flow method; the average execution time is just about 0.147 times the traditional AC power flow method. The larger the system, the shorter will be the execution time. Consequently, we conclude that the overall performance of the proposed approach is sufficient for real-time applications for managing power systems online. In real-time applications, if loading of the transmission line is larger than SIL (surge impedance loading), it will affect the accuracy of the proposed approach; besides, it is worth noting that greater error in bus voltage calculation occurs for large changes in system load demand. If the error is unacceptable, the base case power flow must be executed again to ensure an acceptable solution. In this paper, the changes of 20% in system demand from base case were simulated, and the degree of error was acceptable.

5. Conclusion

In this paper, a hybrid approach composed of the Newton–Raphson method and dynamic programming was proposed for calculating line flow and bus voltage in real time. The proposed method overcomes the convergence problem of the traditional AC power flow method without any iteration after load demand changes, thereby eliminating convergence problem in real-time applications. The voltage magnitude and phase angle at each bus in power systems can be calculated easily with the proposed method, thus reflecting changes in line flows into bus voltages. Numerical results show that the voltage magnitude and phase angle calculated by the proposed approach are nearly the same as those calculated by the AC power flow method. The proposed approach demonstrates high accuracy and short execution time in calculating the bus voltage. Thus, the proposed method is suitable for real-time applications.

Table II. Maximum mismatch of the proposed approach compared with the traditional AC power flow method

Bus voltage / test system	Voltage magnitude (pu) Bus number	Voltage magnitude (pu) Max. error	Phase angle (Degree) Bus number	Phase angle (Degree) Max. error
IEEE 14-bus	10	0.00253	14	0.0700
IEEE 25-bus	24	0.00690	14	0.1771
IEEE 30-bus	30	0.00179	30	0.0630

Table III. Execution time of the proposed approach compared with the traditional AC power flow method

	Traditional AC power flow method (with iteration)		Proposed approach (without iteration)	
Test system	Execution time	Normalized time	Execution time	Normalized time
IEEE 14-Bus	109 ms	1.0	15 ms	0.138
IEEE 25-Bus	180 ms	1.0	32 ms	0.178
IEEE 30-Bus	172 ms	1.0	23 ms	0.134

Appendix

Figure 2 shows a schematic diagram of the transmission line m from bus p to bus q, in which the active and reactive power flow can be expressed as

$$P_m = G_m|V_p|^2 - G_m|V_p||V_q|\cos(\delta_p - \delta_q) - B_m|V_p||V_q|\sin(\delta_p - \delta_q) \tag{A1}$$

$$Q_m = -B_m|V_p|^2 + B_m|V_p||V_q|\cos(\delta_p - \delta_q) - G_m|V_p||V_q|\sin(\delta_p - \delta_q) \tag{A2}$$

where P_m and Q_m denote the active and reactive power flow on arbitrary line m; $|V_p|$, $|V_q|$, and δ_p, δ_q denote the voltage magnitude and phase angles for bus p and q; and G_m and B_m represent the conductance and acceptance of line m.

The active power flow of line m can be modeled as the base-case active power flow (P_m^0) plus the incremental active power flow (ΔP_m), i.e.

$$P_m \cong P_m^0 + \Delta P_m \tag{A3}$$

Furthermore, the incremental active power flow of line m can be modeled as

$$\Delta P_m = \sum_{i=1}^{NB} \frac{\partial P_m}{\partial P_i}\Delta P_i + \sum_{i=1}^{NB} \frac{\partial P_m}{\partial Q_i}\Delta Q_i \tag{A4}$$

These terms can be replaced by $F_p(m,i)$, and $K_p(m,i)$, termed the active power JBDF. Consequently, (A4) can be rewritten as:

$$\Delta P_m = \sum_{i=1}^{NB} F_p(m,i)\Delta P_i + \sum_{i=1}^{NB} K_p(m,i)\Delta Q_i \qquad \text{(A5)}$$

Substituting from (A4) for ΔP_m in (A3), we get

$$P_m \cong P_m^0 + \sum_{i=1}^{NB} F_p(m,i)\Delta P_i + \sum_{i=1}^{NB} K_p(m,i)\Delta Q_i \qquad \text{(A6)}$$

Additionally, the active power JBDF terms can be expressed as

$$F_p(m,i) = \sum_{j=1}^{NB} \frac{\partial |V_j|}{\partial P_i}\cdot\frac{\partial P_m}{\partial |V_j|} + \sum_{j=1}^{NB} \frac{\partial \delta_j}{\partial P_i}\cdot\frac{\partial P_m}{\partial \delta_j} \quad m = 1,2,\ldots,NL \qquad \text{(A7)}$$

And

$$K_p(m,i) = \sum_{j=1}^{NB} \frac{\partial |V_j|}{\partial Q_i}\cdot\frac{\partial P_m}{\partial |V_j|} + \sum_{j=1}^{NB} \frac{\partial \delta_j}{\partial Q_i}\cdot\frac{\partial P_m}{\partial \delta_j} \quad m = 1,2,\ldots,NL \qquad \text{(A8)}$$

where *NL* denotes the number of lines in the system. In (A7) and (A8), the partial differential terms $\frac{\partial |V_j|}{\partial P_i}$, $\frac{\partial \delta_j}{\partial P_i}$, $\frac{\partial |V_j|}{\partial Q_i}$, and $\frac{\partial \delta_j}{\partial Q_i}$ can be calculated in the Jacobian matrix of the base-case power flow solution. In the Newton–Raphson algorithm, the iterative power flow equations can be expressed as

$$\begin{bmatrix} \Delta P \\ \Delta Q \end{bmatrix} = \begin{bmatrix} J_1 & J_2 \\ J_3 & J_4 \end{bmatrix} \begin{bmatrix} \Delta \delta \\ \Delta |V| \end{bmatrix} \qquad \text{(A9)}$$

Moreover, the inverse form of the above equations can be written as

$$\begin{bmatrix} \Delta \delta \\ \Delta |V| \end{bmatrix} = \begin{bmatrix} JB_1 & JB_2 \\ JB_3 & JB_4 \end{bmatrix} \begin{bmatrix} \Delta P \\ \Delta Q \end{bmatrix} \qquad \text{(A10)}$$

in which JB_1 is the term of $\frac{\partial \delta}{\partial P}$. JB_2 is the term of $\frac{\partial \delta}{\partial Q}$, JB_3 is the term of $\frac{\partial |V|}{\partial P}$, and JB_4 is the term of $\frac{\partial |V|}{\partial Q}$. In the base-case power flow solution, these terms can be calculated using the Newton power flow program, which is kept constant during real-time computation when load levels deviate from base case loading conditions. Because line m is from bus p to bus q, active power flow P_m is only related to $|V_p|$,$|V_q|$, δ_p, and δ_q. Therefore, the summation of the differential terms in (A7) and (A8) can be reduced to

$$\begin{aligned} F_p(m,i) = {} & \left(\frac{\partial |V_p|}{\partial P_i}\right)\cdot\frac{\partial P_m}{\partial |V_p|} + \left(\frac{\partial |V_q|}{\partial P_i}\right)\cdot\frac{\partial P_m}{\partial |V_q|} \\ & + \left(\frac{\partial \delta_p}{\partial P_i}\right)\cdot\frac{\partial P_m}{\partial \delta_p} + \left(\frac{\partial \delta_q}{\partial P_i}\right)\cdot\frac{\partial P_m}{\partial \delta_q} \qquad \text{(A11)} \end{aligned}$$

$$\begin{aligned} K_p(m,i) = {} & \left(\frac{\partial |V_p|}{\partial Q_i}\right)\frac{\partial P_m}{\partial |V_p|} + \left(\frac{\partial |V_q|}{\partial Q_i}\right)\frac{\partial P_m}{\partial |V_q|} \\ & + \left(\frac{\partial \delta_p}{\partial Q_i}\right)\frac{\partial P_m}{\partial \delta_p} + \left(\frac{\partial \delta_q}{\partial Q_i}\right)\frac{\partial P_m}{\partial \delta_q} \qquad \text{(A12)} \end{aligned}$$

The derivation of reactive power JBDF is similar to active power JBDF; the reactive power flow of line m can be expressed as

$$Q_m = Q_m^0 + \Delta Q_m \qquad \text{(A13)}$$

The incremental reactive power flow of line m can be expressed as

$$\Delta Q_m = \sum_{i=1}^{NB} \frac{\partial Q_m}{\partial P_i}\Delta P_i + \sum_{i=1}^{NB} \frac{\partial Q_m}{\partial Q_i}\Delta Q_i \qquad \text{(A14)}$$

in which the partial differential terms $\frac{\partial Q_m}{\partial P_i}$ and $\frac{\partial Q_m}{\partial Q_i}$ represent the sensitivity of bus i to line m, from bus p to bus q. These terms can be replaced by $F_q(m,i)$ and $K_q(m,i)$, termed the reactive power JBDF. Accordingly, (A14) can be rewritten as

$$\Delta Q_m = \sum_{i=1}^{NB} F_q(m,i)\Delta P_i + \sum_{i=1}^{NB} K_q(m,i)\Delta Q_i \qquad \text{(A15)}$$

Substituting (A15) for ΔQ_m in (A13), we get

$$Q_m \cong Q_m^0 + \sum_{i=1}^{NB} F_q(m,i)\Delta P_i + \sum_{i=1}^{NB} K_q(m,i)\Delta Q_i \qquad \text{(A16)}$$

Therefore, the reactive power JBDF terms can be derived as follows:

$$F_q(m,i) = \sum_{j=1}^{NB} \frac{\partial |V_j|}{\partial P_i}\cdot\frac{\partial Q_m}{\partial |V_j|} + \sum_{j=1}^{NB} \frac{\partial \delta_j}{\partial P_i}\cdot\frac{\partial Q_m}{\partial \delta_j} \quad m = 1,2,\ldots,NL \qquad \text{(A17)}$$

and

$$K_q(m,i) = \sum_{j=1}^{NB} \frac{\partial |V_j|}{\partial Q_i}\cdot\frac{\partial Q_m}{\partial |V_j|} + \sum_{j=1}^{NB} \frac{\partial \delta_j}{\partial Q_i}\cdot\frac{\partial Q_m}{\partial \delta_j} \quad m = 1,2,\ldots,NL \qquad \text{(A18)}$$

In (A17) and (A18), the partial differential terms $\frac{\partial |V_j|}{\partial P_i}$, $\frac{\partial \delta_j}{\partial P_i}$, $\frac{\partial |V_j|}{\partial Q_i}$, and $\frac{\partial \delta_j}{\partial Q_i}$ can be calculated in the Jacobian matrix of the base-case power flow solution. As mentioned above, the summation of the differential terms in (A17) and (A18) can be curtailed to

$$\begin{aligned} F_q(m,i) = {} & \left(\frac{\partial |V_p|}{\partial P_i}\right)\cdot\frac{\partial Q_m}{\partial |V_p|} + \left(\frac{\partial |V_q|}{\partial P_i}\right)\cdot\frac{\partial Q_m}{\partial |V_q|} \\ & + \left(\frac{\partial \delta_p}{\partial P_i}\right)\cdot\frac{\partial Q_m}{\partial \delta_p} + \left(\frac{\partial \delta_q}{\partial P_i}\right)\cdot\frac{\partial Q_m}{\partial \delta_q} \qquad \text{(A19)} \end{aligned}$$

$$\begin{aligned} K_q(m,i) = {} & \left(\frac{\partial |V_p|}{\partial Q_i}\right)\frac{\partial Q_m}{\partial |V_p|} + \left(\frac{\partial |V_q|}{\partial Q_i}\right)\frac{\partial Q_m}{\partial |V_q|} \\ & + \left(\frac{\partial \delta_p}{\partial Q_i}\right)\frac{\partial Q_m}{\partial \delta_p} + \left(\frac{\partial \delta_q}{\partial Q_i}\right)\frac{\partial Q_m}{\partial \delta_q} \qquad \text{(A20)} \end{aligned}$$

Acknowledgments

The authors are grateful for financial support from the Ministry of Science and Technology, Taiwan, under Grant MOST 104-3113-E-042A-004-CC2.

References

(1) Scott B. Review of load-flow calculation methods. *Proceedings of the IEEE* 1974; **62**(**7**):916–929.
(2) Tinney WF, Hart CE. Power flow solution by Newton's method. *IEEE Transactions on Power Apparatus and Systems* 1967; **PAS-86**:1449–1456.
(3) Stott B, Alsac O. Fast decoupled load flow. *IEEE Transactions on Power Apparatus and Systems* 1974;**PAS-93**,(**3**):859–869.
(4) Kamel S, Jurado F. Fast decoupled load flow analysis with SSSC power injection model. *IEEJ Transactions on Electrical and Electronic Engineering* 2014; **9**(**4**):370–374.
(5) Kamel S, Abdel-Akher M, Jurado F. Improved NR current injection load flow using power mismatch representation of PV bus. *International Journey of Electric Power and Energy System* 2013; **53**(**1**):64–68.
(6) Yang XY, Zhou XX, Ma YC, Du ZC. Asymptotic numerical method for continuation power flow. *International Journey of Electric Power and Energy System* 2012; **43**(**1**):670–679.

(7) de Moura AP, de Moura AAF. Newton–Raphson power flow with constant matrices: a comparison with decoupled power flow methods, *International Journey of Electric Power and Energy System* 2013; **46**(**1**):108–114.
(8) Wood AJ, Wollenberg BF. *Power Generation, Operation and Control.* Wiley: New York; 1996.
(9) Ng WY. Generalized generation distribution factors for power system security evaluations. *IEEE Transactions on Power Apparatus and Systems* 1981; **100**(**1**):1001–1105.
(10) Lin CE, Chen ST, Huang CL. A two-step sensitivity approach for real-time line flow calculation. *Electric Power Systems Research* 1991; **21**(**1**):63–69.
(11) Chang YC, Yang WT, Liu CC. A new method for calculating loss coefficients. *IEEE Transaction on Power Systems* 1994; **9**(**3**): 1665–1671.
(12) Chang YC, Yang WT, Liu CC. Improvements on the line outage distribution factor for power system security analysis. *Electric Power Systems Research* 1993; **26**(**1**):231–236.
(13) Lin CE, Chen ST, Huang CL. A direct Newton-Raphson economic dispatch. *IEEE Transaction on Power Systems* 1992; **7**(**3**):1149–1154.
(14) Ruiz PA, Sauer PW. Voltage and reactive power estimation for contingency analysis using sensitivites. *IEEE Transaction on Power Systems* 2007; **22**(**2**):639–647.
(15) Huang WT, Yao KC. New network sensitivity-based approach for real-time complex power flow calculation. *IET Generation Transmission & Distribution* 2012; **6**(**2**):109–120.
(16) Burns RM, Gibson CA. Optimization of priority lists for a unit commitment program. IEEE Power Engineering Society Summer Meeting, Paper A-75-453-1, 1975.
(17) Liu W. A heuristic dynamic programming based power system stabilizer for a turbo generator in a single machine power system. *The 38th IAS Annual Meeting Industry Applications Conference 2003* 2003; **1**(**1**):270–276.
(18) Lew M. *Dynamic Programming. Studies in Computational Intelligence.* **3.** Springer: Berlin and Heidelberg; 2007.
(19) Power systems test case archive. http://www.ee.washington.edu/research/pstca/.

Wei-Tzer Huang (Non-member) was born in Taiwan, Republic of China, on August 15, 1971. He received the B.S., M.S., and Ph.D. degrees in Electrical Engineering from the National Taiwan University of Science and Technology, Taipei, Taiwan, in 1997, 1999, and 2005, respectively. Presently, he is an Associate Professor with the National Changhua University of Education. His research interests include modeling and simulation of power systems, microgrid modeling and online management, and power electronics.

Kai-Chao Yao (Non-member) was born in Chang-hua, Taiwan, Republic of China, on November 4, 1971. He entered the Electrical Engineering Department of the National Taipei Institute of Technology in 1990. He obtained the bachelor's and master's degrees from the University of New Haven, USA, both in Electrical Engineering, in 1997 and 1998, respectively, and the Ph.D. degree in Electrical and Computer Engineering from Wichita State University, USA, in 2000. Currently, he is a Professor with the Department of Industrial Education and Technology, National Changhua University of Education, Taiwan. His research interests include electrical engineering, virtual instrument technology, and industrial education.

Chun-Ching Wu (Non-member) was born in Taiwan, Republic of China, on January 13, 1971. He received the M.S. degree in Electrical Engineering from Chien-Kuo University of Technology, Changhua, Taiwan, in 2009. Presently, he is pursuing the Ph.D. degree in Department of Industrial Education and Technology, National Changhua University of Education. His research interests include modeling and simulation of power systems.